Observation of a Hot High-Current Electron Beam from a Self-Modulated Laser Wakefield Accelerator

M. I. K. Santala,[1,4] Z. Najmudin,[1] E. L. Clark,[1] M. Tatarakis,[1] K. Krushelnick,[1] A. E. Dangor,[1] V. Malka,[2] J. Faure,[2] R. Allott,[3] and R. J. Clarke[3]

[1]*Plasma Physics Group, The Blackett Laboratory, Imperial College, London SW7 2BZ, United Kingdom*
[2]*LULI, CNRS-CEA, École Polytechnique–Université Pierre et Marie Curie, 91128 Palaiseau Cedex, France*
[3]*Central Laser Facility, Rutherford Appleton Laboratory, Chilton OX11 0QX, United Kingdom*
[4]*Department of Engineering Physics and Mathematics, Helsinki University of Technology, P.O. Box 2200, 02015 HUT, Finland*

(Received 25 May 2000)

A highly relativistic electron beam produced by a 50 TW laser-plasma accelerator has been characterized by photonuclear techniques. The beam has large divergence that increases with plasma density. The electron yield also increases with plasma density and reaches up to 4×10^{11} electrons (>10 MeV), with beam current approaching the Alfvén limit. Effective electron temperatures exceeding 8 MeV are found, leading to an order of magnitude higher photonuclear activation yield than in solid target experiments with the same laser system.

DOI: 10.1103/PhysRevLett.86.1227 PACS numbers: 52.38.–r, 25.20.–x, 52.75.Di

Very underdense plasmas produced by intense ($>10^{19}$ W/cm^2) subpicosecond laser pulses are potentially efficient sources of high-energy electrons [1,2]. High intensity laser pulses can produce large amplitude plasma waves with longitudinal electric field exceeding 100 GV/m [3]. These can produce electrons with energies up to 100 MeV using sources with dimensions on the order of 1 mm (e.g., Refs. [4,5]).

Self-modulated laser wakefield acceleration (LWFA) has recently been the most studied means of generating energetic electrons [2–5]. In moderately dense plasmas (electron density $n = 10^{19}$ cm^{-3}, $\approx$1% of critical density) very large accelerating fields can be generated as plasma waves reaching wave breaking amplitudes are driven through forward Raman scattering and self-modulation of the focused laser pulse in the plasma [2,6].

Direct laser acceleration (DLA) is another mechanism recently identified in 3D particle-in-cell (PIC) simulations [7] and observed in experiments at a moderate power [8]. It occurs due to betatron oscillations of electrons in the quasistatic fields generated during the interaction. Simulations suggest that this process may be as efficient as the LWFA in some situations.

The physics of these acceleration mechanisms is not yet fully understood so experimental measurements of the high-energy electrons are important. For applications, it is also necessary to characterize the electron beams in terms of energy spectrum, electron yield, and beam divergence (emittance). Until now, these properties have been studied simultaneously only in a few experiments. In particular, there are no measurements of total relativistic electron yields and no measurements of the electron beam divergence at high electron energies and with high laser power. Some electron beam profiles at low energy have been measured (e.g., in Refs. [8–10]) and several authors have provided spectral information but these are typically measured on axis and with a small acceptance angle (e.g., Refs. [3,4]).

In this paper we characterize the electron beam produced in a high power (50 TW) gas jet experiment at different plasma densities by photonuclear activation techniques previously used in laser-solid interaction studies [11–13]. This is a single-shot, full-beam technique that is well adapted for the low repetition rate of high-energy, short-pulse lasers. As the diagnostic is completely insensitive to energies below reaction thresholds (8–22 MeV) only electrons with energies in excess of this contribute to our activation results. We measure simultaneously the yield, spectrum ("temperature"), and divergence of the energetic electrons. The total electron current is shown to be close to the Alfvén limit. Compared to laser-solid experiments with the same laser, an order of magnitude increase in the photonuclear activation yield is observed.

The experiment was carried out at Rutherford Appleton Laboratory using the high power, short-pulse beam of the Vulcan laser [14]. The laser operates at 1.05 μm and provides up to 50 J of energy to target with <1 ps pulse length. The linear-polarized beam could be converted to circular polarization by inserting a $\lambda/4$ plate in the beam. The target was a helium gas jet produced by a supersonic nozzle (diameter 4 mm). The jet has a very homogeneous density profile and a sharp edge [15]. The laser beam was focused at the front edge of the jet by an off-axis paraboloidic mirror in $f/4$ geometry resulting in an estimated intensity up to 10^{19} W/cm^2. The experimental conditions are similar to Ref. [4], but the laser power is higher. Several plasma diagnostics were employed: Raman forward scattering (RFS) was measured with a near-infrared sensitive spectrometer, the plasma was imaged by transverse probe beam shadowgraphy, as well as by spectrally resolved self-side scatter. Plasma density vs gas jet pressure was calibrated using the frequency shift of Stokes

and anti-Stokes lines in the RFS spectra. The density was varied in the range $(0.5-4.5) \times 10^{19}$ cm^{-3}. Besides activation, electrons were measured also by a magnetic spectrometer.

The activation target (Fig. 1) consisted of 1 mm of tantalum (Ta) as a bremsstrahlung converter and a main activator made of 13 copper (Cu) pieces in a 10 mm thick layer covering a solid angle of 0.3 sr. A 3 mm layer of polytetrafluoroethylene [PTFE, $(CF_2)_n$] was used as an additional activator on several shots. Radiochromic film (RCF) was placed in front of the Ta layer as a monitor sensitive to all electron energies. The high-energy electrons produce bremsstrahlung with good efficiency in the Ta converter and to some extent in Cu. Bremsstrahlung is directed in a narrow cone along the direction of the incident electrons, so only the copper pieces in that direction are exposed. Some of the bremsstrahlung photons induce nuclear reactions in the target materials (Table I). As the different reactions are sensitive to different energies, spectral information (temperature) can be deduced by measuring several reactions simultaneously. Background due to secondary $(n, 2n)$ reaction is estimated to be negligible as it has 11 MeV threshold and low probability above this.

Activity of the β^+ decaying nuclides was measured by coincidence counting with two standard 75 mm NaI(Tl) detectors (see Ref. [13] for a description of the setup). The other nuclides were measured by a 25% efficient n-type germanium detector within a 10 cm thick lead shield. The γ spectra were recorded and analyzed by a PC-based multichannel analyzer. Typical counting times were 100 s for the coincidence setup and 1000 s for the Ge detector. All results were corrected for decay.

The angular distributions were determined by measuring the ^{62}Cu activity in each copper segment at different plasma densities. Two measured, normalized distributions and the observed width (FWHM) as a function of plasma density are shown in Fig. 2. It is seen that electrons are emitted in a fairly wide beam and the cone angle increases with plasma density. The angle is found to be only weakly sensitive to the laser power.

The yield of ^{61}Cu ($\gamma, 2n$ reactions) was generally too low to allow it to be used for a piecewise angular distribution measurement. On some high-yield shots at high density the ^{61}Cu activity was measured separately for the three to four central copper pieces and the four pieces surrounding these. The ratio of these activities was compared to the corresponding ratio from the ^{62}Cu measurements and no significant difference was observed. Consequently, the angular distribution of highly relativistic electrons does not appear to be very energy dependent.

The behavior of divergence in our measurements differs from previous results [9] where narrowing of low-energy electron emission was observed as the laser power and the plasma density were increased. The likely reason is that the laser power is around the threshold of relativistic guiding in Ref. [9] (8 TW) while in this work it is greatly exceeded. Hence we expect more complicated beam propagation effects like filamentation and beam breakup to occur [17]. The divergence we observe cannot be explained by space-charge expansion alone as a divergence of only 1°–2° (FWHM) is expected at the highly relativistic

TABLE I. Nuclear reactions used. Q is the reaction threshold, σ_{max} is the peak cross section, $T_{1/2}$ is the half-life of the reaction product, and γ:s are the main radiation energies [16].

Reaction	Q (MeV)	σ_{max} (mb)	$T_{1/2}$	γ:s (keV)
^{63}Cu$(\gamma, n)^{62}$Cu	10.9	75	9.7 m	511[a]
^{63}Cu$(\gamma, 2n)^{61}$Cu	19.7	13	3.3 h	283, 656; 511[a]
^{181}Ta$(\gamma, n)^{180}$Ta	7.6	350	8.2 h	93, 104
^{181}Ta$(\gamma, 3n)^{178}$Ta	22.1	20	2.4 h	213, 326, 426
^{12}C$(\gamma, n)^{11}$C	18.7	9	20 m	511[a]
^{19}F$(\gamma, n)^{18}$F	10.5	10	110 m	511[a]

[a]Positron annihilation radiation.

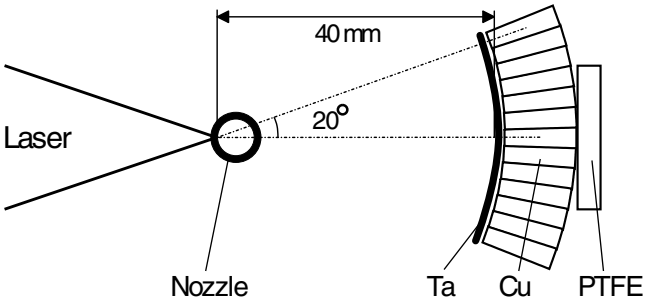

FIG. 1. Schematic drawing of the target setup.

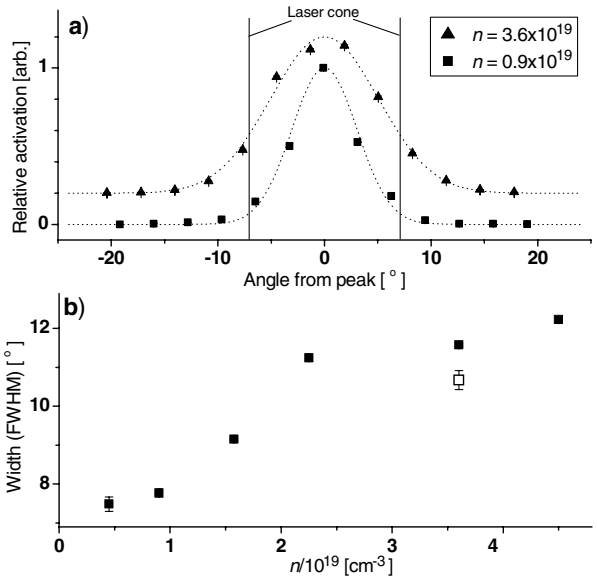

FIG. 2. (a) Normalized angular distributions measured with ^{62}Cu activation for a low (squares) and a high plasma density (cm^{-3}), offset for clarity. The lines indicate a Gaussian fit to data. 0° is approximately the direction of the laser beam. (b) Width (FWHM) of the electron beam as a function of plasma density. Energy on target was 25–45 J, except a low-energy shot (open square) that was 10 J.

energies [9,18]. The divergence could signal a change in the predominant acceleration mechanism from LFWA to DLA as a large transverse momentum is predicted for DLA [7]. Other possible causes include filamentation, hosing of the laser and electron beams [19,20], and plasma lensing [21].

To deduce the initial number of electrons and their spectrum the slowing down of the electrons and generation of bremsstrahlung in the target materials was modeled numerically. The total and radiative energy loss were modeled by data from the ESTAR database [22] and the bremsstrahlung spectrum was modeled using data by Seltzer and Berger [23]. The incident electrons were assumed to have a quasithermal energy spectrum $f(E) = f_0 \exp(-E/kT)$. This is a reasonable assumption as seen in magnetic spectrometer measurements (Fig. 3 and Refs. [4,8]) and as well as in several PIC simulations [7]. The calculated bremsstrahlung spectrum was folded with the reaction cross sections [16] to estimate the activation yield of each reaction at different "effective" temperatures T. Matching the ratio of measured yields of two reactions in one material to these estimates gives T, and f_0 can then be found from the absolute yield.

The effective electron temperatures were determined separately from the measured ^{61}Cu/^{62}Cu, ^{11}C/^{18}F, and ^{178}Ta/^{180}Ta activity ratios. These differ in a consistent fashion from shot to shot. The average effective electron temperatures for shots with a large activation yield are 8.2 MeV for Cu and 10.8 MeV for C/F. For Ta, a lower value of 4.4 MeV is obtained. However, this could be skewed by, for example, uneven activation distribution and self-absorption effects. A large population of electrons at relatively low energies as predicted by Tzeng *et al.* [24] could also explain the result. In tantalum, the main finding is the repeated observation of ^{178}Ta, with the reaction Q value of 22 MeV and a cross section peaking at 25–30 MeV (Fig. 4).

There is clear evidence of temperature increase with increasing laser power at constant density (Fig. 5a). This figure also indicates that at lower densities the temperature of the electrons increases with density but beyond about 2×10^{19} cm^{-3} there is a slight decrease. The results show an increasing coupling of the laser energy to the hot electrons, with an eventual saturation which is consistent with the onset of wave breaking [3].

The electron yield (above 10 MeV) was also estimated using the quasithermal model. For high-energy, high density shots the yield was $(1.5–3.8) \times 10^{11}$ electrons while lowest yields were about 10^{10}. To produce enough bremsstrahlung to explain the largest ^{178}Ta activation, $10^9–10^{10}$ electrons must be at or above 40 MeV. Assuming a 1 ps bunch duration [25], the beam current ($E > 10$ MeV) is up to 60 kA and the total current about 200 kA (with $T = 8$ MeV). This is approaching the Alfvén limit (350 kA at 10 MeV). Consequently, the self-induced magnetic field can have a major impact on the propagation of the low-energy (below a few MeV's) electrons, and plasma lensing may affect the divergence of the high-energy electrons. This agrees well with the fact that wide patterns were observed on the RCF.

The total energy carried by the fast electrons was up to 1 J with peak conversion efficiency exceeding 2%. The conversion efficiency is plotted in Fig. 5b, and the increase with plasma density is clear. The measured efficiency is in reasonable agreement with PIC simulations in Ref. [24], which predict 10% total efficiency and 1% above 25 MeV. Laser beam polarization did not affect the yield. This would suggest that electrons are not trapped into the wake by Raman backscattering since less efficient trapping is predicted with circular polarization [26].

The large electron and activation yields suggest that laser-plasma accelerators (if operating at a high-repetition rate) could be applied to produce short-lived radioactive sources. In high density shots, the typical total ^{62}Cu activity produced was 10–20 kBq [$(1–2) \times 10^7$ nuclei], and the highest observed was 30 kBq. In low density shots, less than 1 kBq was produced. The yields are much higher

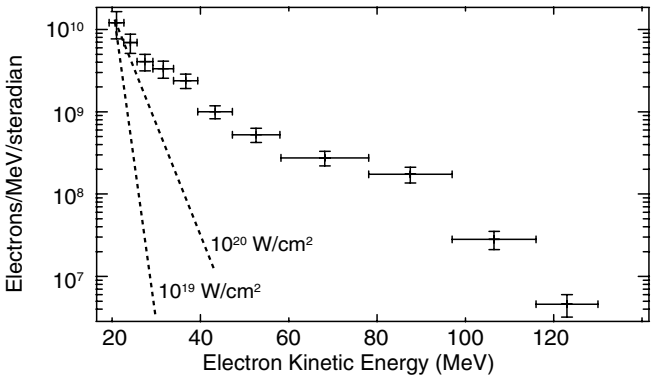

FIG. 3. A typical electron spectrum (unfolded) measured by an on-axis electron spectrometer. Ponderomotive scalings (Ref. [12]) at 10^{19} and 10^{20} W/cm^2 are also shown.

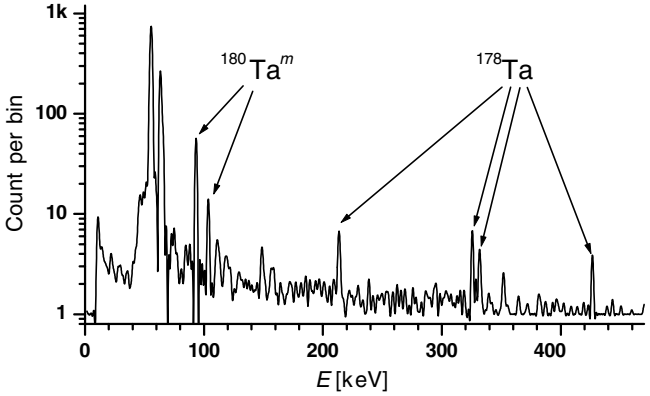

FIG. 4. A typical γ spectrum measured from the activated Ta samples (smoothed and offset by 1, integration time 2000 s, and 1 bin = 0.163 keV). The characteristic gamma lines of ^{180}Ta^m (93 and 104 keV) and ^{178}Ta (213, 326, 332, and 426 keV) are clearly observed. The other lines originate from Hf/Ta/W x rays or natural background.

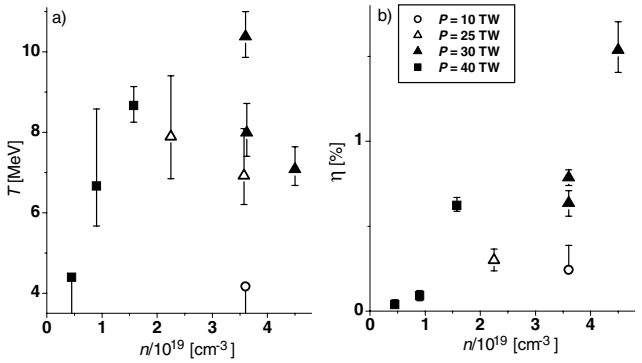

FIG. 5. (a) Measured (Cu activation) temperatures at different plasma densities and laser powers. (b) Energy conversion efficiency from laser energy to electrons above 10 MeV.

than in solid-target experiments using Vulcan, where typically <1 kBq was observed [13]. The number of ^{62}Cu nuclei we observe is higher than that of ^{238}U fissions as reported in Petawatt experiments [12], yet the Cu cross section is smaller and the threshold higher. The efficient activity production results from the hotter electron distribution in the LWFA that leads to more efficient production of very energetic bremsstrahlung. This would suggest another application in time-resolved hard x-ray radiography [27].

It is of interest to note that the plasma acceleration in large, homogeneous, highly underdense plasma leads to temperature and photonuclear activation yield that are on par with the highest intensity laser-solid experiments [12], and these have been achieved with only a fraction of the laser energy. The high measured temperature is strong evidence that the energetic electrons are produced by an acceleration mechanism and not merely by ponderomotive force. A self-focused intensity of 10^{21} W/cm^2 would be needed to explain the measured spectra. However, at high laser power, self-focusing does not produce a single highly intense channel but the beam breaks into several filaments each having an intensity below 10^{20} W/cm^2 [17]. We have measured the self-focused peak intensity of $\approx 5 \times 10^{19}$ W/cm^2 under similar conditions [28].

One of the main observations in this paper is that the electron divergence increases with increasing plasma density already in the very underdense regime. This could be detrimental for the fast ignitor scheme [29], where the fast electrons are generated in fairly dense plasma. Efficient underdense acceleration could also result in an energy spectrum that is too hot for localized energy deposition.

In conclusion, we have characterized the electron beam produced by the self-modulated LWFA in terms of electron yield, temperature, and divergence by photonuclear activation techniques. We have measured up to 4×10^{11} electrons above 10 MeV having a characteristic temperature of about 8 MeV. We have observed that the angular spread of the emitted electron beam increases with plasma density but appears to saturate. The total yield of fast electrons is found to increase with plasma density. The total photonuclear activation yield is found to be more than an order of magnitude more than in solid-target experiments with similar laser parameters, which is of particular interest for potential applications.

The authors acknowledge the excellent support of all the Central Laser Facility staff and the useful discussions with K. Ledingham and I. Spencer. This work was supported by EPSRC grants (No. GR/K93815 and No. GR/L04498), and M. I. K. S. was financed by the EU TMR network SILASI (No. ERBFMRX-CT96-0043) and Jenny ja Antti Wihurin Rahasto.

[1] T. Tajima and J. M. Dawson, Phys. Rev. Lett. **43**, 267 (1979); T. Tajima and P. Chen, Nucl. Instrum. Methods Phys. Res., Sect. A **410**, 344 (1998).
[2] E. Esarey *et al.,* IEEE Trans. Plasma Sci. **24**, 252 (1996).
[3] A. Modena *et al.,* Nature (London) **377**, 606 (1995).
[4] D. Gordon *et al.,* Phys. Rev. Lett. **80**, 2133 (1998); C. E. Clayton *et al.,* Phys. Rev. Lett. **81**, 100 (1998).
[5] C. I. Moore *et al.,* Phys. Rev. Lett. **79**, 3909 (1997); D. Umstadter *et al.,* Science **273**, 472 (1996).
[6] P. Sprangle *et al.,* Phys. Rev. Lett. **69**, 2200 (1992); E. Esarey *et al.,* Phys. Fluids B **5**, 2690 (1993).
[7] A. Pukhov and J. Meyer-ter-Vehn, Phys. Plasmas **5**, 1880 (1998); A. Pukhov, Z.-M. Sheng, and J. Meyer-ter-Vehn, *ibid.* **6**, 2847 (1999).
[8] C. Gahn *et al.,* Phys. Rev. Lett. **83**, 4772 (1999).
[9] R. Wagner *et al.,* Phys. Rev. Lett. **78**, 3125 (1997).
[10] C. I. Moore *et al.,* Phys. Rev. E **61**, 788 (2000).
[11] M. H. Key *et al.,* Phys. Plasmas **5**, 1966 (1998); S. P. Hatchett *et al., ibid.* **7**, 2076 (2000); K. W. D. Ledingham *et al.,* Phys. Rev. Lett. **84**, 899 (2000).
[12] T. E. Cowan *et al.,* Phys. Rev. Lett. **84**, 903 (2000).
[13] M. I. K. Santala *et al.,* Phys. Rev. Lett. **84**, 1459 (2000).
[14] C. N. Danson *et al.,* J. Mod. Opt. **45**, 1653 (1998).
[15] V. Malka *et al.,* Rev. Sci. Instrum. **71**, 2329 (2000).
[16] EXFOR and NUDAT on-line databases at http://www-nds.iaea.org
[17] A. Chiron *et al.,* Phys. Plasmas **3**, 1373 (1996).
[18] S. Humphries, *Charged Particle Beams* (Wiley, New York, 1990).
[19] K.-C. Tzeng *et al.,* Phys. Plasmas **6**, 2105 (1999); B. J. Duda *et al.,* Phys. Rev. Lett. **83**, 1978 (1999).
[20] Z. Najmudin *et al.*, in *Proceedings of the Conference on Inertial Fusion Sciences and Applications 99,* edited by C. Labaune *et al.* (Elsevier, Paris, 2000), p. 409.
[21] J. J. Su *et al.,* Phys. Rev. A **41**, 3321 (1990).
[22] Estar on-line database at http://physics.nist.gov
[23] S. Seltzer and M. Berger, At. Data Nucl. Data Tables **35**, 345 (1986).
[24] K. C. Tzeng *et al.,* Phys. Rev. Lett. **79**, 5258 (1997).
[25] A. Ting *et al.,* Phys. Rev. Lett. **77**, 5377 (1996); S. P. Le Blanc *et al., ibid.* **77**, 5381 (1996).
[26] E. Esarey *et al.,* Phys. Rev. Lett. **80**, 5552 (1998).
[27] M. D. Perry *et al.,* Rev. Sci. Instrum. **70**, 265 (2000); T. Goldsack *et al.* (to be published).
[28] K. Krushelnick *et al.,* Phys. Rev. Lett. **83**, 737 (1999).
[29] M. Tabak *et al.,* Phys. Plasmas **1**, 1626 (1994).